Appl. Phys. B 80, 459–462 (2005)
DOI: 10.1007/s00340-005-1737-1

Applied Physics B
Lasers and Optics

E. WU
H. PAN
S. ZHANG
H. ZENG✉

High power single-longitudinal-mode operation in a twisted-mode-cavity laser with a c-cut Nd:$GdVO_4$ crystal

Key Laboratory of Optical and Magnetic Resonance Spectroscopy, and Department of Physics, East China Normal University, Shanghai 200062, People's Republic of China

Received: 26 July 2004 / Revised version: 25 November 2004
Published online: 18 February 2005 •

ABSTRACT A twisted-mode-cavity laser was established by using a piece of c-cut Nd:$GdVO_4$ crystal as the laser's active material. Output spectra were scanned by a scanning Fabry–Perot interferometer, which demonstrated that the single-longitudinal-mode laser operation was realized in the twisted-mode-cavity laser configuration. A maximum single-longitudinal-mode laser output power of 2.1 W was obtained when the pump power was 11.5 W. The pump slope efficiency was about 20.0%. A passively Q-switched single-longitudinal-mode laser was also achieved in a twisted-mode cavity by inserting a piece of Cr^{4+}:YAG as an intracavity saturable absorber. The Q-switched single-longitudinal-mode laser pulse duration was measured to be 100 ns and the single-pulse energy was about 40.0 μJ.

PACS 42.55.Xi; 42.55.Rz; 42.60.Gd

1 Introduction

Single-longitudinal-mode (SLM) operation of diode-pumped solid-state lasers attracts a lot of interest for various applications, such as coherent lidars, coherent optical communications, high-resolution spectroscopy, and so on. As already known, in the common standing-wave lasers, and especially high-power solid-state lasers, spatial hole-burning in active gain materials usually causes multimode laser operation. Various techniques have been tried to obtain SLM laser operation. SLM operations can be achieved in microchip lasers with extraordinarily thin gain materials, owing to the large frequency interval between adjacent longitudinal modes in the relevant laser cavities. Nevertheless, microchip lasers are not capable of high-power output because of the thinness of the gain material. Laser operation in a ring laser cavity is another well known technique to obtain SLM output, wherein an intracavity optical diode keeps unidirectional laser propagation so that no standing-wave electric fields are formed in the cavity, leading to the elimination of spatial hole-burning in the active material. But traditional ring lasers generally consist of several mirrors [1, 2], which makes them hard to adjust. Another solution to obtain SLM operation is to eliminate the troublesome spatial hole-burning by employing a twisted-mode cavity (TMC), which was first introduced by Etuhov and Siegman in 1965 [3]. Compared with the normal standing-wave cavity, a TMC laser contains several polarization elements in the cavity to control the polarization state of the intracavity beam. A Brewster plate is placed in front of the output mirror to select a certain oscillating polarization and a pair of quarter-wave plates (QWPs) sandwich the laser's active material. The principal axes of the QWPs are oriented with their fast axes perpendicular or parallel to each other and at 45° to the direction of polarization selected by the Brewster plate [4]. SLM laser operation has been achieved in TMC lasers with active gain media such as Yb-ion and Nd-ion doped materials [4–7]. However, a TMC laser cannot be achieved with anisotropic laser crystals since it requires that there should be no birefringence along the resonator axis in the laser material. Generally speaking, TMC lasers can only be achieved with the isotropic crystals, such as Nd:YAG, since anisotropy of the active material's polarization-dependent gain may bring about incomplete elimination of spatial hole-burning under the standard TMC configuration. In order to get a laser gain independent of the laser polarization direction to establish a TMC laser with an anisotropic crystal, Louyera et al. chose a c-cut Nd:YLF as the gain material [5], which gave a clue for TMC laser design with an anisotropic crystal. However, the absorption band of Nd:YLF is around 796 nm, which goes slightly beyond the standard wavelength for commercially available diodes. As a result, they could not make full advantage of the diode pumping. At present, the popular diode-pumped laser crystal Nd:YVO_4 is not favorable for a TMC laser because it is of critical importance that the gain media should possess negligible thermal birefringence to get a stable single-mode output from a TMC laser. Those strict requirements limit the application of TMC lasers under high-power diode laser pumping, where either thermal birefringence or anisotropic laser crystals may break the TMC configuration. Thus, it is still a challenge to operate single-mode TMC lasers for diode-pumped Nd:YVO_4 lasers.

Recently, a new laser crystal, Nd:$GdVO_4$, has been developed, which is suitable for high-power laser-diode pumping.

✉ Fax: +86-21-62232056, E-mail: hpzeng@phy.ecnu.edu.cn

Besides its absorption band of about 1.6 nm at 808.4 nm [8], which matches well with the emission band of a GaAlAs laser diode, Nd:GdVO$_4$ possesses a large absorption cross-section that is even larger than Nd:YVO$_4$, making it quite suitable to take full advantage of laser-diode pumping. Compared with Nd:YVO$_4$, Nd:GdVO$_4$ exhibits a much higher thermal conductivity (11.7 W/mK along the <110> direction [9]), even comparable to that of Nd:YAG, which enables it to be high-power pumped [10–14]. Also, owing to its large thermal conductivity, the thermal birefringence in the Nd:GdVO$_4$ crystal is weak. The thermal expansion coefficient is 7.42×10^{-6}/K along the <001> direction and 1.05×10^{-6}/K along the <100> direction, which is much smaller than that of Nd:YVO$_4$ (11.37×10^{-6}/K and 4.43×10^{-6}/K, respectively). And the temperature coefficient of birefringence of the Nd:GdVO$_4$ crystal is measured to be also as low as 4.33×10^{-6}/K [15]. The good thermal properties, especially the weak thermal birefringence, make this newly developed crystal suitable for high-power laser diode pumping and TMC laser operation.

Moreover, a crystal employed in a TMC laser must have some necessary characteristics in its structure. As an isomorph of YVO$_4$, the GdVO$_4$ crystal belongs to the group of oxide compounds crystallizing in a Zircon structure with a tetragonal space group. It is a positive uniaxial crystal with the optical axis parallel to the c-axis. In order to achieve TMC operation in a Nd:GdVO$_4$ laser, the crystal should be oriented with the c-axis parallel to the laser axis; that is to say, a c-cut crystal should be used in the TMC laser so as to make sure no birefringence would be induced when the laser beam passes through the crystal.

In this paper, we demonstrate experimentally that SLM operation can be achieved in a continuous wave (cw), as well as a Q-switched TMC laser with a c-cut Nd:GdVO$_4$ crystal under high-power laser diode pumping, which verified the birefringence induced by thermal effects under high-power laser-diode pumping, producing negligible influence on the c-cut Nd:GdVO$_4$ TMC laser. This paper is organized as follows. After this short introduction, we describe our experiments and experimental results in Sect. 2. Both cw and Q-switched TMC lasers are discussed. Section 3 gives a brief conclusion.

2 Experiments and discussions

The resonator configuration of the TMC laser is shown in Fig. 1. In our experiments, a 13-W fiber-coupled diode-laser array was used as the pump source. The output wavelength of the diode-laser array was centered at 808 nm when controlled by thermal regulation at room temperature.

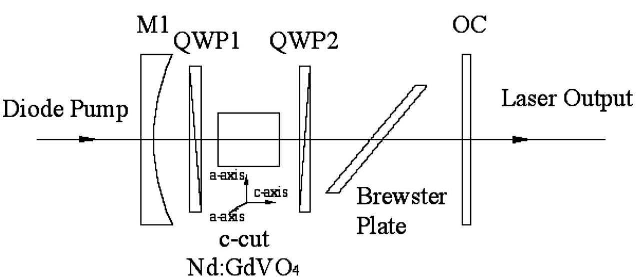

FIGURE 1 Twisted-mode-cavity (TMC) Nd:GdVO$_4$ laser setup

The fiber core had a diameter of 400 μm and a numerical aperture of 0.22. The pump laser beam was focused by two pieces of aspheric lenses on the Nd:GdVO$_4$ crystal. And the resonator was composed of one concave mirror and one flat output coupler. The input concave mirror M1 ($R = 500$ mm) was covered with an antireflection coating at 808 nm and a high-reflection coating at 1064 nm. The output coupler had a transmittance of 5% at 1064 nm, which was optimized by the comparison of laser outputs obtained with output couplers of different transmittances. We used two pieces of zero-order wave-plates with an antireflection coating at 1064 nm on both sides to sandwich the c-cut Nd:GdVO$_4$ crystal. The Brewster plate was a piece of 0.5-mm-thick fused silica. The total cavity length was about 80 mm.

The laser crystal was wrapped with indium foil and set in a water-cooled copper heat sink. We chose a piece of 1.0 at.% doped 3-mm-long c-cut Nd:GdVO$_4$ as the laser's active material, which was antireflection coated at 808 nm and 1064 nm on both sides. Although the c-cut Nd:GdVO$_4$ crystal has a lower stimulated emission cross-section ($\sigma_g = 1.2 \times 10^{-19}$ cm^2) compared with the a-cut crystal ($\sigma_g = 7.6 \times 10^{-19}$ cm^2), which leads to a higher threshold, the c-cut Nd:GdVO$_4$ laser has a higher slope efficiency because the intrinsic loss of the c-cut Nd:GdVO$_4$ crystal is smaller than that of the a-cut one [16, 17]. This was confirmed by the Findlay-clay analysis in our experiment [18]. The output couplers with different transmittances of 5, 10, 15, 20, 25 and 30% were employed in our experimental measurements, and the a-cut Nd:GdVO$_4$ crystal used for experimental comparison was also 1.0-at.%-doped, 3-mm-long, and antireflection-coated on both sides. The cavities for both the c-cut crystal laser and the a-cut one were exactly the same. The Findlay-clay analysis results are displayed in Fig. 2, where the round-trip losses are shown as the absolute values of the intercepts on the x axis. It was indicated that the round-trip loss of the c-cut crystal (0.01) was smaller than that of the a-cut one (0.05). Especially, the c-cut Nd:GdVO$_4$ crystal is favorable for generating high single-pulse energy in the passively Q-switched lasers because the lower emission cross-section of the c-cut Nd:GdVO$_4$ can better satisfy the criterion for a good passive Q-switching [16].

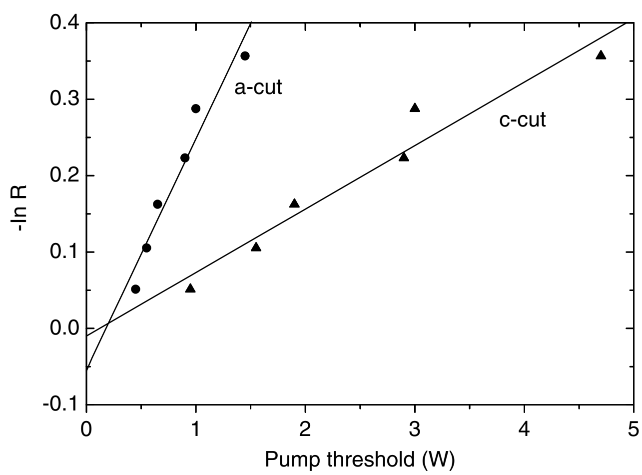

FIGURE 2 The Findlay-Clay analysis in our experiments showed that the round-trip loss of the c-cut Nd:GdVO$_4$ crystal was smaller than that of the a-cut one

The analysis of the intracavity polarization helps us to understand the SLM operation in the TMC laser. The cooperation of the intracavity QWPs and the Brewster plate keeps two counter-propagating orthogonally circularly-polarized laser beams traveling in the laser's active material. The overlapped electronic field vector can be expressed as:

$$E = \begin{bmatrix} E_0 e^{-i(kz-\pi/2)} + E_0 e^{-i(2kL-kz-\pi/2)} \\ E_0 e^{-ikz} + E_0 e^{-i(2kL-kz-\pi)} \end{bmatrix} \quad (1)$$

Here, the two components of the electric field vector are along the axis of the QWP, and $k = 2\pi/\lambda$ (λ is the wavelength of the laser), while z is the beam position along the resonator axis and L represents the optical length of the laser cavity. Then, the light intensity along the axis in the crystal can be calculated:

$$I = E_x^2 + E_y^2 \sim 4E_0^2 \quad (2)$$

where I is the light intensity in the crystal, and E_x and E_y stand for the electric field vectors along the two orthogonal axes, respectively. It is evident that the light intensity is independent of the beam position z along the resonator axis. Consequently, the laser beam has a spatially uniform light intensity along the resonator axis in the gain material; that is to say, there is no spatial hole-burning along the axis and the laser will oscillate in the SLM. As indicated in this brief analysis, a TMC laser operation requires that there exist no birefringence effects in the laser's active crystal. In this case, a c-cut $Nd:GdVO_4$ laser could meet this requirement. Before setting it into the laser cavity, we placed the crystal between two crossed polarizers as a check and we found that no birefringence occurred.

Without any polarization elements positioned inside the resonator, the c-cut $Nd:GdVO_4$ laser operated at a multi-longitudinal-mode oscillation. Under such a multimode operation, a maximum output power of 4.0 W was obtained at the incident pump power of 11.5 W, and the slope efficiency was as high as 39.8%. The output laser was polarized and the polarization ratio was about 7:1. When the QWPs and Brewster plate were inserted into the cavity, an SLM laser operation was attained by carefully adjusting the intracavity polarization elements, such as QWP 1 and the Brewster plate. To monitor the output spectra, we used a Fabry–Perot interferometer, which could scan over a range of 3 GHz—approximately three free spectral ranges of the laser cavity. Figure 3 lays out the output spectra resolved by using such a Fabry–Perot scanning interferometer. Figure 3a shows the output spectrum of the $Nd:GdVO_4$ laser in an ordinary standing-wave cavity, i.e., without QWPs in the cavity. The output was multimode because of the existence of spatial hole-burning in the $Nd:GdVO_4$ laser's active material. Figure 3b shows the output spectrum of the TMC $Nd:GdVO_4$ laser. SLM operation was observed. The polarization ratio of the output beam was about 53:1.

When the incident pump power on the crystal was increased, the TMC laser tended to run at the transverse multimode operation. The transverse multimode operation might be caused by the mismatch between the pump and the oscillating laser modes in the laser crystal, which caused the high-order transverse modes to oscillate. However, by carefully aligning the cavity, the laser output would return to the SLM state with still high output power (~2.1 W) and at the TEM_{00} transverse mode. The transverse mode of the output laser was checked by a pinhole detection system, which indicated that lasers with or without TMC ran at single-transverse mode when they were operated at the maximum output power. The M^2 value of the TMC laser at the maximum pumping power was measured to be 2.01, while $M^2 = 1.98$ without TMC configuration. Figure 4 shows the SLM laser output power of the TMC laser as a function of the incident pump power. The threshold and slope efficiency of the TMC laser were 1.1 W and 20%, respectively. At the maximum pump power, we obtained a maximum SLM laser output of 2.1 W from this TMC laser. Since we set up the experiment in an open cavity, there were several factors that influenced the SLM operation, such as the air current and mechanic instability of the laser cavity, and the SLM operation tended to be slightly unstable due to the

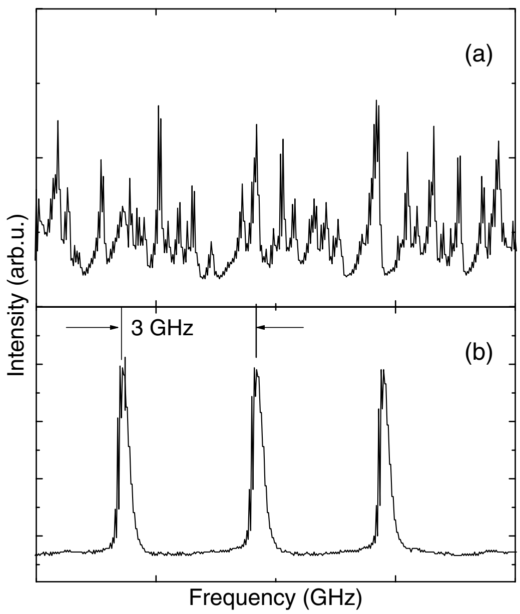

FIGURE 3 Output spectra resolved by using a scanning Fabry–Perot interferometer with a free spectral range of 3 GHz. **a** A standard standing-wave $Nd:GdVO_4$ laser and **b** a TMC $Nd:GdVO_4$ laser

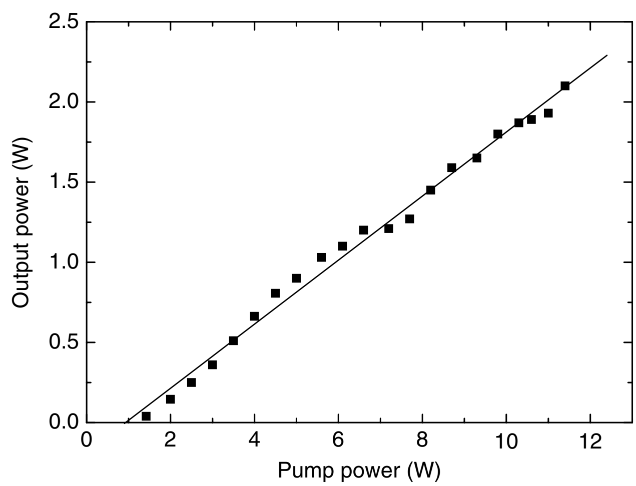

FIGURE 4 Single-longitudinal-mode (SLM) laser output power of the TMC laser as a function of pump power

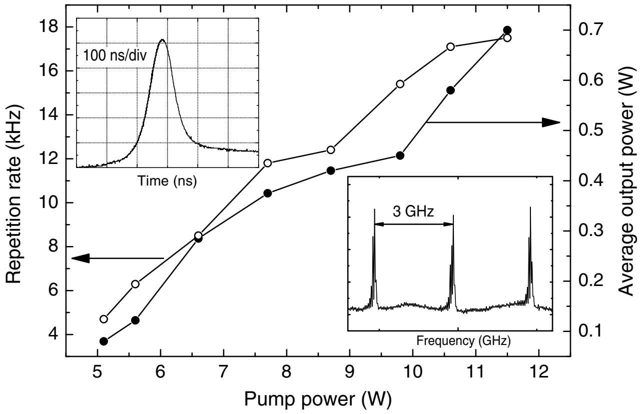

FIGURE 5 Pulse repetition rate and average output power of the Q-switched laser versus pump power. *Inset*: output spectrum of the Q-switched pulse

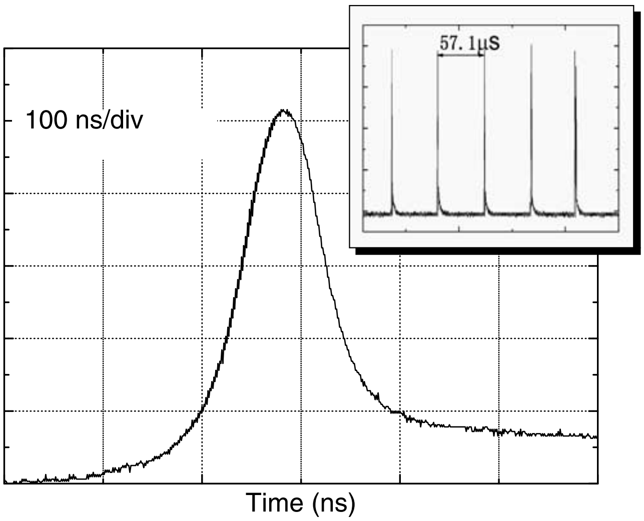

FIGURE 6 Oscilloscope trace of the Q-switched pulse. *Inset*: the corresponding laser pulse repetition rate was recorded to be 17.5 kHz

competition of the adjacent longitudinal modes. To get a stable SLM operation in this TMC $Nd:GdVO_4$ laser, further stabilization is needed, for instance, by using fringe side locking [6].

Q-switched laser pulses of SLM operation could also be obtained in this TMC $Nd:GdVO_4$ laser by inserting a piece of saturable absorber into the cavity. In this case, a piece of Cr^{4+}:YAG crystal worked as the passive Q-switch. Since YAG is a kind of isotropic crystal, it produces no influence on the intracavity laser polarization. In our experiment, a Cr^{4+}:YAG crystal with an initial transmittance of 90% and an antireflection coating at 1064 nm on both sides was inserted between the Brewster plate and the output coupler. The threshold of this passively Q-switched SLM laser increased to 5.1 W due to the loss of the passive Q-switch. At the highest available pump power (11.5 W), the maximum attainable energy for a single Q-switched pulse was 40.0 μJ under the SLM operation. The repetition rate of the pulsed laser was 17.5 kHz. Figure 5 shows the Q-switched pulse repetition rate and the average output power versus the pump power. The repetition rate and the average output power increased with the pump power. The inset shows the SLM output spectrum. Under different pump powers, the pulse duration remained almost the same, about 100 ns, as shown in Fig. 6. The oscilloscope trace of the Q-switched laser pulse was recorded when the maximum output power was achieved with the repetition rate of 17.5 kHz, as shown in the inset. Note that such a passively Q-switched SLM laser can be more compact if the Cr^{4+}:YAG is uncoated and tilted at a Brewster angle to function as a passive Q-switch and Brewster plate.

3 Conclusions

In summary, we demonstrated, for the first time, a diode-pumped high-power single-longitudinal-mode (SLM) $Nd:GdVO_4$ laser in a twisted-mode cavity (TMC). Although $Nd:GdVO_4$ is a positive uniaxial crystal and TMC operation cannot be achieved in a commonly-used a-cut crystal laser, we realized SLM continuous-wave (cw) and Q-switched lasers in a TMC configuration with c-cut $Nd:GdVO_4$ crystals as the intracavity active gain media, which verified that the c-cut $Nd:GdVO_4$ crystal possessed negligible birefringence induced by thermal effects under high-power laser-diode pumping.

ACKNOWLEDGEMENTS This work was partly supported by the Key Project from the Science and Technology Commission of Shanghai Municipality (grant 04dz14001), the National Key Project for Basic Research (grant TG1999075204), and the National Natural Science Fund (grant 60478011).

REFERENCES

1 X. Li, Q. Pan, J. Jing, C. Xie, K. Peng, Opt. Commun. **201**, 165 (2002)
2 M.V. Okhapkin, M.N. Skvortsov, A.M. Belkin, S.N. Bagayev, Opt. Commun. **194**, 207 (2001)
3 V. Etuhov, A.E. Siegman, Appl. Opt. **4**, 142 (1965)
4 D.A. Draegert, IEEE J. Quantum Electron. **8**, 235 (1972)
5 Y. Louyera, F. Balemboisb, M.D. Plimmera, T. Badra, P. Georgesb, P. Juncara, M.E. Himbert, Opt. Commun. **217**, 357 (2003)
6 C.S. Adams, J. Vorberg, J. Mlynek, Opt. Lett. **18**, 420 (1993)
7 T.Y. Fan, J. Ochoa, IEEE Photonics Technol. Lett. **7**, 235 (1995)
8 T. Jensen, V. Ostroumov, J. Meyn, G. Huber, A. Zagumennyi, I. Shcherbakov, Appl. Phys. B **58**, 373 (1994)
9 P.A. Studennikin, A.I. Zagumennyi, Y.D. Zavartsev, P.A. Popov, I.A. Shcherbakov, Quantum Electron. **25**, 1162 (1995)
10 J. Liu, B. Ozygus, S. Yang, J. Erhard, U. Seelig, A. Ding, H. Weber, X. Meng, L. Zhu, L. Qin, C. Du, X. Xu, Z. Shao, J. Opt. Soc. Am B **20**, 652 (2003)
11 B. Zhang, G. Li, M. Chen, Z. Zhang, Y. Wang, Opt. Lett. **28**, 1829 (2003)
12 J. He, C. Lee, J. Huang, S. Wang, C. Pan, K. Huang, Appl. Opt. **42**, 5496 (2003)
13 A. Agnesi, A. Guandalini, G. Reali, S. Dell'Acqua, G. Piccinno, Opt. Lett. **29**, 56 (2004)
14 S. Zhang, E. Wu, H. Pan, H. Zeng, IEEE J. Quantum Electron. **QE-40**, 505 (2004)
15 L.J. Qin, X.L. Meng, H.Y. Shen, L. Zhu, B.C. Xu, L.X. Huang, H.R. Xia, P. Zhao, G. Zheng, Cryst. Res. Technol. **38**, 793 (2003)
16 J. Liu, J. Yang, J. He, Opt. Commun. **219**, 317 (2003)
17 Y. Chen, Y. Lan, Appl. Phys. B **74**, 415 (2002)
18 D. Findlay, R.A. Clay, Phys. Lett. **20**, 277 (1966)